Determination of the Predominant Ionization and Loss Mechanisms for the Low-Voltage Arc Mode in a Neon Plasma Diode*

S. N. SALINGER† AND J. E. ROWE

Electron Physics Laboratory, Department of Electrical Engineering, The University of Michigan, Ann Arbor, Michigan

(Received 27 March 1967; in final form 30 April 1968)

A reaction-rate analysis is used to determine the relative importance of the predominant ionization and loss mechanisms in a neon low-voltage arc. Experimental data are derived from various experiments to determine density, cross section, etc. It is found that the resonance and metastable state atoms are primarily generated in a region near the cathode which corresponds to the "cathode ball-of-fire" region of the low-voltage arc. The predominant ion-generation process is found to be a result of collisions between excited atoms which cause the formation of a molecular ion. Direct ionization of ground-state atoms is of secondary but non-negligible, importance. Consideration of quasi-equilibrium multistage ionization shows that, unlike the cesium low-voltage arc, it is unimportant in the neon low-voltage arc. The escape of resonance radiation accounts for approximately one-fifth of the total power loss while ionization accounts for approximately one-eighth. Most of the remaining power loss appears as power dissipation at the anode.

I. INTRODUCTION

Much effort has been devoted in recent years to studies of the ionization and loss mechanisms in cesium-filled plasma diodes and thermionic converters,[1–6] and a fairly clear picture of the predominant mechanisms in the ignited, or low-voltage arc, mode has begun to emerge. It has fairly conclusively been shown that the plasma in an ignited-mode cesium thermionic converter is in a state of Saha equilibrium so that the predominant ionization mechanism is multiple-step ionization via the many possible excited states of cesium.[4–6] It also has been shown that the cross section for the formation of molecular ions from excited atoms in cesium is too small for this mechanism to account for an appreciable fraction of the ionization in ignited-mode thermionic converters.[7]

Much less work has been done on the ionization and loss mechanisms of the low-voltage arc mode in noble-gas plasma diodes. The results available[8–11] are based upon work performed prior to the recent advances in atomic collision physics and cesium thermionic converters. As with the early work on cesium diodes, the early studies on noble-gas low-voltage arcs have proposed both direct and two-stage ionization as being predominant. These investigations have also attributed a wide variety of importances to the various loss mechanisms possible in this type of discharge including excitation, ionization, radiation, recombination and diffusion. In view of the recent evidence which has forced modification of the earlier theories of the cesium low-voltage arc, it seems desirable to reexamine the behavior of noble-gas low-voltage arcs to determine whether the same ionization and loss mechanisms are responsible for their behavior as govern the behavior of the low-voltage arc mode in cesium diodes. The present study is directed toward answering this question.

In this analysis reliable Langmuir-probe data are combined with detailed atomic-physics data to obtain information not available solely from either an experimental or theoretical analysis on reaction rates for the processes in question. A low-voltage arc in neon is analyzed because complete atomic-physics data for neon is available. Also, it is then possible to make use of the extensive experimental data of Martin and Rowe[12] for the spatial variation of the plasma potential, electron density, and electron temperature in a neon-filled plasma diode operating in the low-voltage arc mode.

II. EXPERIMENTAL DATA BASE

The experimental configuration used by Martin and Rowe consisted of a parallel-plane diode with an 0.75-in. diam impregnated-matrix-type cathode and a 4-in.-diam molybdenum anode. The cathode was surrounded by a 4-in. diam planar stainless steel guard ring at cathode potential. The electrode spacing was variable from about 0.5 to 5 cm. The cathode temperature was generally held at 1100°C, which produced a saturated cathode emission of 10 A/cm^2. The diode was contained in a stainless steel ultrahigh vacuum chamber of 8-in. i.d. which was baked and pumped to 1×10^{-8} Torr prior to admission of the working gas. Research-grade inert gases were used throughout. All plasma measure-

* This work was supported by the U.S. Army Electronics Command.

† Present address: Sylvania Electronic Systems, Mountain View, Calif.

[1] H. L. Witting and E. P. Gyftopoulos, J. Appl. Phys. **36,** 1328 (1965).

[2] D. H. Pollock and A. O. Jensen, J. Appl. Phys. **36,** 3184 (1965).

[3] H. L. Witting, *Proceedings of the Thermionic Conversion Specialist Conference, Houston, Texas,* (Nov. 1966), p. 75.

[4] D. R. Wilkins and E. P. Gyftopoulos, J. Appl. Phys. **37,** 2892 (1966).

[5] B. Y. Moizhes *et al.*, Sov. Phys.—Tech. Phys. **10,** 1252 (1966).

[6] W. H. Reichelt, *Proceedings of the Conference on Thermionic Electrical Power Generation, London,* (Sept. 1965).

[7] A. G. F. Kniazzeh, *26th Annual Conference on Physics Electronics, Cambridge, Mass.* (March 1966), p. 1.

[8] K. T. Compton, Phys. Rev. **20,** 283 (1922).

[9] G. Holst and E. Oosterhuis, Physica **4,** 42 (1924).

[10] M. J. Druyvesteyn, Z. Physik **64,** 781 (1930).

[11] E. O. Johnson, RCA Rev. **16,** 498 (1955).

[12] R. J. Martin and J. E. Rowe, J. Appl. Phys. (to be published).

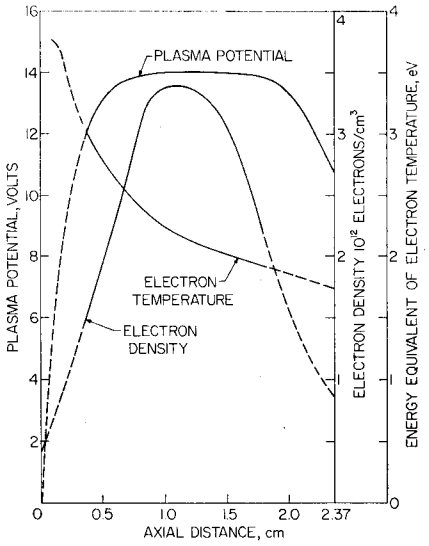

FIG. 1. Experimental behavior of the plasma diode being analyzed. Axial profiles of plasma potential, electron density and electron temperature. (Neon at $p=2$ Torr, $I=4$ A, $d=2.37$ cm) (from Martin and Rowe.[12])

ments were taken using pulsed and shielded Langmuir probes. Care was taken in all areas to insure stable and reproducible performance. The results obtained are considered to be highly reliable.

Martin has investigated the low-voltage arc mode in neon, argon, and xenon, and has found that in each case there is a minimum value of the pressure-electrode spacing product for which the discharge can exist in this mode. For neon, the low-voltage arc mode could not be sustained below about $pd=2$ Torr·cm, nor would it operate at spacings of less than 1 cm. In every instance,

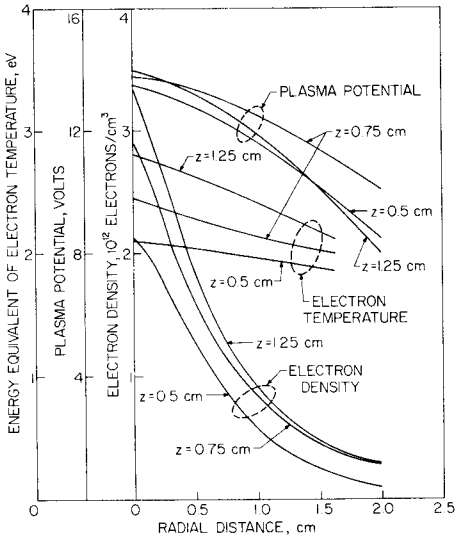

FIG. 2. Experimental behavior of the plasma diode being analyzed. Radial profiles of the plasma potential electron density and electron temperature. (Neon at $p=2$ Torr, $I=4$ A, $d=2.37$ cm) (from Martin and Rowe.[12])

the high-density portion of the discharge was smaller in diameter than the cathode, and could not be made to expand to the full cathode diameter. *Thus, the low-voltage arc mode in noble gases is decidedly two-dimensional, in contrast to cesium where the lower pd products required lead to one-dimensional plasma distributions.*

The data of Martin and Rowe to which the present analysis was applied are shown in Figs. 1 and 2, while the appearance of the discharge is indicated in Fig. 3. The operating conditions of the discharge were pressure $p=2$ Torr, discharge current $I=4$ A, diode spacing $d=2.37$ cm, space-charge-limited cathode emission, and neutral gas temperature $T=300$°C.

III. THE QUASI-EQUILIBRIUM HYPOTHESIS

In view of the recent results on ignited-mode cesium plasma diodes, the first hypothesis to check in relation to the ionization and loss mechanisms in the neon low-

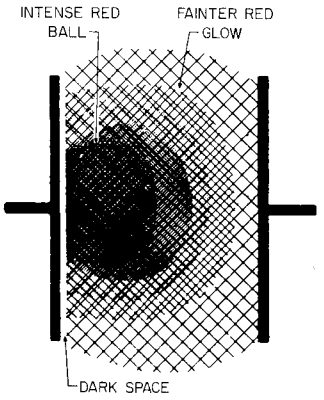

FIG. 3. Visual appearance of the low-voltage arc mode in a planar neon-filled plasma diode.

voltage arc is that of quasi-equilibrium, leading to multistage ionization and three-body recombination. Under quasi-equilibrium there is a local balance between the ionization and loss rates at each point in the plasma and this leads to a local relation between the electron density n_e and temperature T_e. This relation is[4]

$$n_e^2=\nu_i/\beta_r=\psi_e^2(T_e)\,(2g_i/g_a)\,(2\pi m_e kT_e/h^2)^{3/2}N \times \exp(-\mathcal{E}_I/kT_e). \quad (1)$$

Here, ν_i is the multistage ionization rate, β_r is the three-body recombination rate, N is the neutral gas density, $\mathcal{E}_I$ is the ground-state ionization energy of the gas and g_i and g_a are the statistical weights of the ground-state ion and atom, respectively. (This factor has a value of 4 for inert gases.) $\psi_e(T_e)$ is a function of the electron temperature, and of the ionization potentials, cross sections, densities, and statistical weights of all the excited states of the gas, which provides a measure of the nearness with which the plasma approaches a state of local thermodynamic equilibrium. If the plasma is in

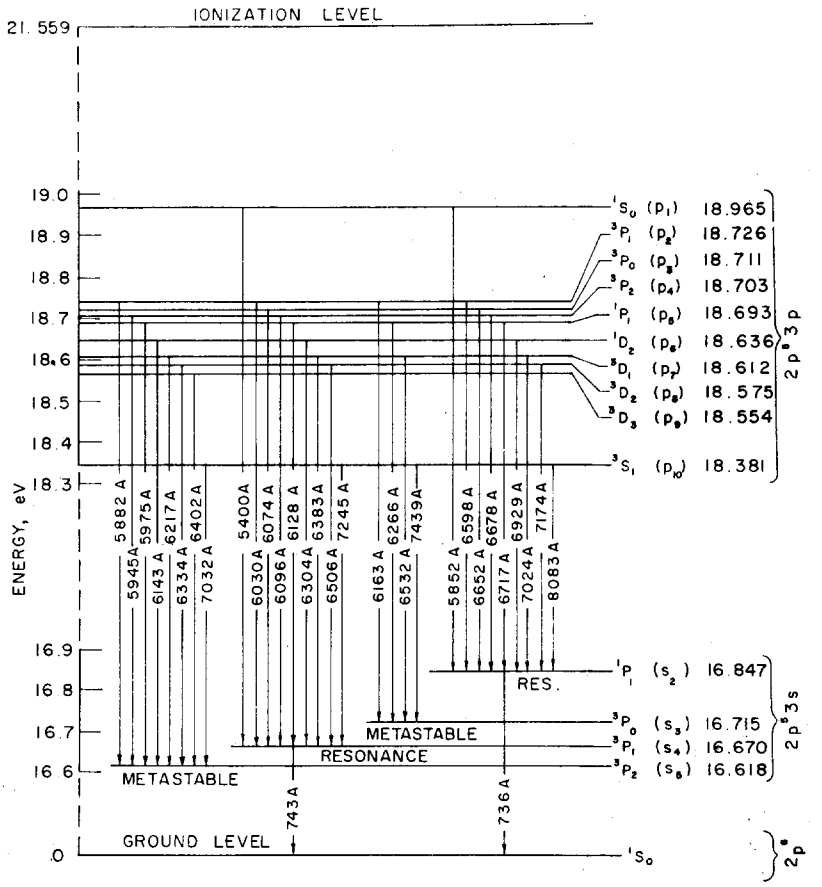

FIG. 4. Energy-level diagram for the first two excited configurations of neon.

local thermodynamic equilibrium with the temperature T_e, then $\psi_e(T_e)=1$, and Eq. (1) is identical with the Saha equation. If some excited states are depleted, then $\psi_e(T_e)<1$ and the quasi-equilibrium density is smaller than that given by the Saha equation. If, on the other hand, $\psi_e(T_e)\ll 1$, then the plasma is not in a state of quasi-equilibrium, and the hypothesis of multistage ionization and three-body recombination is not valid.

To assess the importance of quasi-equilibrium multistage ionization in the neon low-voltage arc under analysis, the measured electron temperatures and densities of Fig. 1 were substituted into Eq. (1), and the result solved for ψ_e. At distances of 0.5, 1.0, and 2.0 cm away from the cathode this led to values of ψ_e of 2.25×10^{-6}, 1.25×10^{-5}, and 1.9×19^{-5}, respectively. Similarly, for a low-voltage arc in xenon studied by Martin the maximum value of ψ_e was found to be 2.7×10^{-3}. The results are in direct contrast to similar computations made by Wilkins and Gyftopoulos[4] on a cesium ignited-mode thermionic converter for which values of $\psi_e\approx1$ were observed for several cases.

The above results indicate that the assumption of quasi-equilibrium in noble-gas low-voltage arcs is completely invalid, so that multistage ionization involving all excited states cannot possibly be of great significance in noble-gas low-voltage arcs. The factors that account for the difference in behavior of cesium and the noble gases in this respect, as seen from Eq. (1), are that cesium low-voltage arcs attain much higher electron densities and much lower electron temperatures than do noble-gas low-voltage arcs. The lower ionization potential of cesium is also significant.

IV. DERIVATION OF THE EXCITED ATOM DENSITY

The failure of the quasi-equilibrium multistage ionization hypothesis for the neon low-voltage arc forces a detailed reexamination of those ionization and loss mechanisms involving the ground state and the lowest excited states. An energy-level diagram for neon, indicating those transitions involving the lowest excited states, is shown in Fig. 4. The first excited configuration of neon (the $2p^53s$ levels) consists of two metastable states ($^3P_0$ and $^3P_2$) and two resonance states ($^3P_1$ and $^1P_1$). All downward transitions to the $3s$ configuration come from the ten $2p^53p$ levels in the next configuration. These transitions produce the red light that is characteristic of neon. The extreme intensity of the spectral lines corresponding to these transitions in the neon low-voltage arc suggests that the $3s$ and $3p$ states play a major role in governing the behavior of the discharge.

Frisch and Revald[13] have shown that the $3p$ states are primarily populated by stepwise excitation from the $3s$ states and that direct excitation from the ground state is negligible by comparison. Photoexcitation of atoms from the $3s$ states to the $3p$ states may also be important, but its effect on any atom is the same as stepwise excitation. The primary loss mechanism for the $3p$ states is spontaneous transition back down to the $3s$ states. Taking all of the $3s$ states as a unit in a rate equation for these states, transition rates to and from the $3p$ states will therefore nearly cancel. Consequently, these processes may be omitted from the rate equation in a first-order determination of the $3s$ state densities.

The rate balance equation for the density of atoms in the $3s$ configuration at steady state is

$$H_A+H_B+H_C+H_D+H_E+H_F=0. \quad (2)$$

Here H_A is the rate of electron-impact excitation of ground-state atoms, given by

$$H_A(\mathbf{x})=N\int_{\mathcal{E}_{ex}}^{\infty} f(\mathcal{E},\mathbf{x})\sigma_{0\to 3s}(\mathcal{E})v(\mathcal{E})\,d\mathcal{E}, \quad (3)$$

where $f(\mathcal{E},\mathbf{x})$ is the electron energy density function, N is the neutral gas atom density, $\sigma_{0\to 3s}(\mathcal{E})$ is the total excitation cross section from the ground state to the $3s$ states, $v(\mathcal{E})=(2\eta(\mathcal{E})^{1/2}$, and $\mathcal{E}_{ex}$ is the threshold energy for excitation.

$H_B(\mathbf{x})$ is the net rate of loss of resonance state atoms from a volume element about point $\mathbf{x}$ by the escape of imprisoned resonance radiation, given by

$$H_B(\mathbf{x})=-\frac{n_R^*(\mathbf{x})}{\tau_R}+\tau_R^{-1}\int_{x'} n_R^*(\mathbf{x}')G(\mathbf{x}',\mathbf{x})d\mathbf{x}'$$
$$\cong-\nu_{IR}n_R^*(\mathbf{x}). \quad (4)$$

Here $n_R^*(\mathbf{x})$ is the density of resonance state atoms at point $\mathbf{x}$, τ_R is the spontaneous emission lifetime of the resonance state, $G(\mathbf{x}',\mathbf{x})$ is the probability that a quantum emitted at $\mathbf{x}'$ is absorbed in a unit volume element around point $\mathbf{x}'$, and ν_{IR} is the decay constant for the decay of imprisoned resonance radiation. The approximation $H_B\cong-\nu_{IR}n_R^*$ follows from assuming that the distribution of excited atoms is close to the fundamental mode for the imprisonment problem and is made to simplify the analysis.

$H_C(\mathbf{x})$ is the reaction rate for deexcitation of metastable atoms in three-body collisions. Phelps[14] has found this to be a probable process and by contrast has found deexcitation through two-body collisions to be highly improbable. $H_C(\mathbf{x})$ is given by $H_C(\mathbf{x})=-\gamma_M N^2 n_M^*(\mathbf{x})$, where γ_M is the three-body collision coefficient and $n_M^*(\mathbf{x})$ is the density of metastable atoms.

$H_D(\mathbf{x})$ is the combined diffusion loss rate for both metastable states, given by

$$H_D(\mathbf{x})=D_M\nabla^2 n_M^*(\mathbf{x})\cong-(D_M/\Lambda_1^2)n_M^*(\mathbf{x}). \quad (5)$$

Here again, the solution to the diffusion problem is approximated by the fundamental mode. D_M is the diffusion coefficient and Λ_1 is the characteristic diffusion length for the first mode of diffusion. Next, $H_E(\mathbf{x})=-Z_E(\mathbf{x})n^*(\mathbf{x})$ is the rate of ionization of $3s$ state atoms by electron impact, with $Z_E(\mathbf{x})$ being the corresponding rate coefficient. Finally, the loss rate due to inelastic collisions between pairs of $3s$ excited atoms is $H_F(\mathbf{x})=-\alpha_S[N^*(\mathbf{x})]^2$, where α_S is the rate coefficient.

Now, let b be the fraction of those atoms in the $3s$ configuration which are in the two metastable states. Thus $n_M^*(\mathbf{x})=bn^*(\mathbf{x})$ and $n_R^*(\mathbf{x})=(1-b)n^*(\mathbf{x})$. Then, substituting the various rates into Eq. (2) and solving for $n^*(\mathbf{x})$ yields

$$n^*(\mathbf{x})=-(B/2\alpha_S)+\{(B/2\alpha_S)^2+[H_A(\mathbf{x})/\alpha_S]\}^{1/2}, \quad (6)$$

where

$$B=Z_E(\mathbf{x})+b[(D_M/\Lambda_1^2)+\gamma_M N^2]+(1-b)\nu_{IR}. \quad (7)$$

V. DETERMINATION OF REACTION RATES

Next it is necessary to determine numerical values for the various terms in Eqs. (6) and (7). First consider $H_A(\mathbf{x})$, as given by Eq. (3). The excitation cross section for neon metastables is determined by normalizing the high-resolution, but unnormalized data of Olmsted[15] to the values obtained from the low-resolution absolute data of Maier–Liebnitz.[16] The results are shown in Fig. 5. The excitation cross section for the resonance states is assumed to be equal to that of the metastable states, so that $\sigma_{0\to 3s}(\mathcal{E})=2\sigma_M(\mathcal{E})$. To simplify the computation, it is assumed that $f(\mathcal{E},\mathbf{x})$ is Maxwellian. Then, considering only the variation along the z axis, data on $n_e(z)$ and $T_e(z)$ are taken from the Martin and Rowe[12] results in Fig. 1 to determine $f(\mathcal{E},z)$; for the conditions $p=2$ Torr and $T=300°$C, N is 3.37×10^{16} atoms/cm^3. To integrate Eq. (3), $\sigma_{0\to 3s}(\mathcal{E})$ is approximated by a series of ramp functions and the result is shown in Fig. 6.

An identical approach is used for calculating $Z_E(z)$, taking the cross-section data of Vriens.[17] The result is shown in Fig. 7.

The value of b will be determined next. Since the mean thermal energy of the neutral gas is of the order of magnitude of the energy separation between the various $3s$ levels, collisions of $3s$ atoms with ground-state atoms will be effective in causing radiationless transitions between the various $3s$ states. Collisions of thermal electrons with $3s$ atoms will also be effective in transferring atoms between $3s$ states since the amount of

[13] S. E. Frisch and V. F. Revald, Opt. Spectrosc. **15**, 395 (1963).
[14] A. V. Phelps, Phys. Rev. **114**, 1011 (1959).
[15] J. Olmsted, III, *et al.*, J. Chem. Phys. **42**, 2321 (1965).
[16] H. Maier-Liebnitz, Z. Physik **95**, 499 (1935).
[17] L. Vriens, Phys. Letters **8**, 260 (1964).

energy that must be converted from kinetic to potential, or vice versa, is small. Using rate coefficients measured by Phelps[14] for the various processes, it was found that in the neon low-voltage arc thermal electrons are far more efficient than ground-state atoms in producing collision-induced transitions between the various $3s$ states. The $3s$ states will therefore be in approximate thermal equilibrium at the electron temperature. Using Boltzmann's law and the energies and quantum statistical weights of the $3s$ states, the relative populations of these states may be estimated. For $kT_e=3.3$ eV, corresponding to the location of the peak in Fig. 6, the fraction of $3s$ atoms in the metastable states is found to be $b=0.6$, while the fraction in the resonance states is $1-b=0.4$.

The diffusion coefficient for neon metastables under the conditions $p=1$ Torr and $T=300°$K, as determined from Phelps's[14] data, is $D_M=136.3$ cm^2/sec, while the three-body collision coefficient is estimated as $\gamma_M\cong10^{-32}$

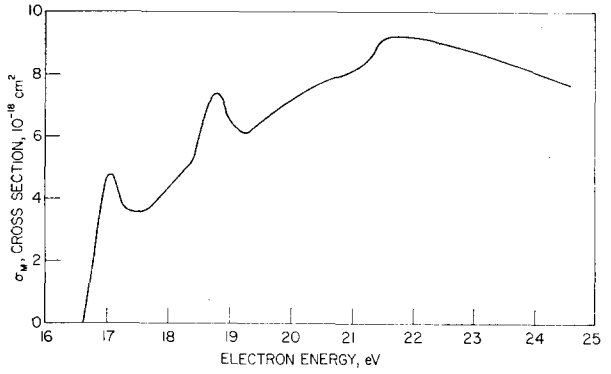

FIG 5. Cross section for the excitation of neon atoms to the $^3P_2$ and $^3P_0$ metastable states by electron impact (adapted from Olmsted *et al.*[15] and Maier-Liebnitz[16]).

cm^6/sec. The diffusion length Λ_1 for the particular discharge under study is estimated to be 0.38 cm and this leads to a diffusion rate per metastable atom of $D_M/\Lambda_1^2=943$ sec^{-1}. The loss rate per metastable atom due to three-body collisions is estimated as $\gamma_M N^2=11.4$ sec^{-1}. Thus, the loss of metastable atoms due to three-body collisions is negligible compared with the loss due to diffusion.

Next, it is necessary to estimate the decay constant ν_{IR} for the imprisoned resonance radiation. ν_{IR} is taken as the weighted average of the values for the two resonance states. Holstein[18] has shown that ν_{IR_j} is of the form $\nu_{IR_j}=g/\tau_{R_j}$. Here g is the "escape factor" which may be regarded as the reciprocal of the average number of emissions and absorptions of an individual quantum of excitation energy prior to its escape from the discharge. τ_{R_j} is the spontaneous-emission lifetime of the jth resonance state. The quantity g depends on the absorptivity of the resonance radiation by the gas, the spontaneous-emission lifetime τ_{R_j}, the geometry of the

[18] T. Holstein, Phys. Rev. **83**, 1159 (1951).

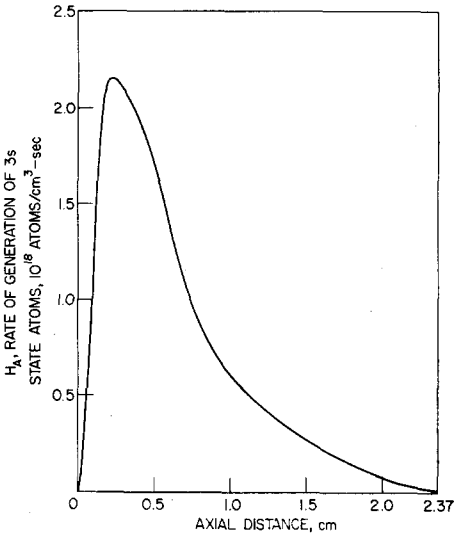

FIG. 6. Axial variation of the rate of generation of $3s$ metastable and resonance state atoms.

enclosure, and the type of spectral line broadening that is predominant.

For the gas pressures, electron densities, and electron temperatures occurring in the low-voltage arc mode, Doppler broadening will be the predominant broadening mechanism. Pressure broadening is relatively unimportant at gas pressures significantly below atmospheric pressure, while for a neon plasma in the range of $n_e\approx10^{12}$ cm^{-3}, $T_e\approx2\times10^4°$K Stark broadening is expected to be small compared with Doppler broadening.[19] For Doppler broadening in a parallel-plane

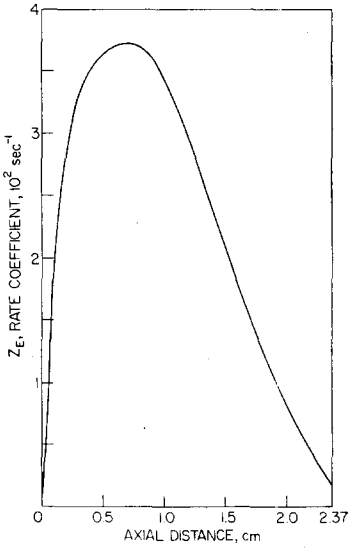

FIG. 7. Rate coefficient for the ionization of $3s$ state atoms as a function of axial position.

[19] W. L. Weise, in *Plasma Diagnostic Techniques*, R. H. Huddlestone and S. L. Leonard, Eds. (Academic Press Inc., New York, 1965), p. 265.

geometry, g is given by[18]

$$g' = 1.875/k_0 L[\pi \ln(k_0 L)]^{1/2}, \quad (8)$$

while for a cylindrical geometry

$$g'' = 1.60/k_0 R[\pi \ln(k_0 R)]^{1/2}. \quad (9)$$

Here k_0 is the absorption coefficient at the center of the resonance line and is given by

$$k_0 = (\lambda_j^3 N/8\pi)(w_{s_i}/w_0)(\pi^{1/2} v_0 \tau_{R_i})^{-1}, \quad (10)$$

where λ_j is the wavelength of the radiation, w_{s_i} and w_0 are, respectively, the quantum-statistical weights of the resonance state and the ground state, and $v_0 = (2kT/M_0)^{1/2}$ is the mean thermal speed of the gas atoms. L and R are the dimensions of a cylindrical region containing most of the excited atoms, here taken as that region over which the rate of generation of atoms in the $3s$ configuration is at least 10% of its peak value, as determined from Figs. 2 and 6.

At the wavelengths of neon resonance radiation ($\simeq$740 Å) the wall reflectivities of the electrodes are under 10%.[20] Cayless[21] has considered the effect of wall reflectivity upon the imprisonment of resonance radiation and has found that for reflectivities of up to 50%, reflection has a negligible effect upon the distribution of resonance atoms. Consequently, it will be assumed that all resonance radiation reaching the electrodes is absorbed and has no further effect on the discharge. The escape factor g will then be taken, to a first approximation, as the sum of the axial and radial escape factors, $g = g' + g''$.

Use of the above equations and approximations, together with published values for the lifetimes of the two resonance states,[22,23] leads to imprisonment decay constants for the given discharge of 10.43×10^4 sec^{-1} for the $^1P_1$ state and 3.72×10^4 sec^{-1} for the $^3P_1$ state. Weighting of these values in proportion to the relative computed densities of the two states at the position of maximum excited atom generation in the discharge leads to a net decay constant for both resonance states of $\nu_{IR} = 5.33 \times 10^4$ sec^{-1}.

Next consider collisions between pairs of excited atoms. Since the combined excitation energy of the two interactants in this type of collision is much larger than the ionization potential of either one, there is an overwhelming probability that the system will seek to reduce its potential energy by undergoing an ionization.

First consider collisions between pairs of metastable atoms. There are two possible mechanisms for this type of interaction:

$$X^m \times X^m \rightarrow X^+ + X + e, \quad (11)$$

and

$$X^m + X^m \rightarrow (X_2^*)_{\text{unstable}} \rightarrow X_2^+ + e. \quad (12)$$

Myers[24] has argued that process (12) will occur in preference to process (11) because the ionization potential of the molecule is less than that of the atom by the value of the binding energy of the molecule. This conclusion is supported by experimental evidence.

Ferguson[25] has developed a classical collision model for the calculation of cross sections for atomic reactions requiring zero activation energy and has obtained good agreement with experiment. Such reactions include collisions between excited atoms in a gas. Ferguson's method has been used here to calculate the cross section for collisions between pairs of neon metastable atoms. To apply Ferguson's method it is necessary to calculate the coefficients for the van der Waals potentials between the possible combinations of interactants. Using the latest available data on neon line strength,[26] the van der Waals coefficients for the possible combinations of colliding neon metastables are found to be $a^{3P_2-3P_2} = 11.48 \times 10^{-58}$ erg·cm^6, $a^{3P_0-3P_0} = 12.96 \times 10^{-58}$ erg·cm^6, and $a^{3P_0-3P_2} = 12.55 \times 10^{-58}$ erg·cm^6.

Using these values, the cross sections for metastable–metastable collisions in neon at 573°K are found to be $\sigma^{3P_2-3P_2} = 1.11 \times 10^{-14}$ cm^2, $\sigma^{3P_0-3P_0} = 1.16 \times 10^{-14}$ cm^2, and $\sigma^{3P_0-3P_2} = 1.14 \times 10^{-14}$ cm^2. These compare favorably with measurements of Phelps and Molnar[27] in helium at 300°K of 10^{-14} cm^2 for two colliding He(2^3S) metastables. This is in sharp contrast with the measured value of 7×10^{-18} cm^2 obtained by Kniazzeh[7] for cesium molecular ion formation by the collision of two resonance-state cesium atoms, and accounts for the great increase in importance of excited atom collisions in noble-gas low-voltage arcs relative to cesium low-voltage arcs.

No attention has been given in the literature to collisions between pairs of noble-gas resonance-state atoms or to collisions between resonance-state atoms and metastable-state atoms. However, if the rate of generation of resonance-state atoms is high, and the resonance radiation is strongly imprisoned, then the density of resonance-state atoms will also be high, and collisions of these types will be very likely. Again, such collisions will most likely result in the formation of molecular ions as in Eq. (12), but with one or both of the metastable atoms replaced by resonance-state atoms. The energy differences and oscillator strengths of the $3p \rightarrow 3s$ transitions terminating on the $^3P_1$ and $^1P_1$ resonance states are very similar to those of the transitions terminating on the $^3P_0$ and $^3P_2$ metastable states. Therefore, it may reasonably be assumed that the cross section for any combination of colliding $3s$ state atoms is nearly equal to the average of the cross sections for

[20] L. R. Koller, *Ultraviolet Radiation* (John Wiley & Sons, Inc., New York, 1965), 2nd ed., pp. 199–215.
[21] M. A. Cayless, *Proceedings of the 6th International Conference on Ionization Phenomena in Gases* (SERMA, Paris, 1963), Vol. 2, p. 155.
[22] A. V. Phelps, Phys. Rev. **100**, 1230 (1955).
[23] F. A. Korolev *et al.*, Opt. Spectrosc. **16**, 304 (1964).
[24] H. Myers, Phys. Rev. **130**, 1639 (1963).
[25] E. E. Ferguson, Phys. Rev. **128**, 210 (1962).
[26] D. W. Koopman, J. Opt. Soc. Am. **54**, 1354 (1964).
[27] A. V. Phelps and J. P. Molnar, Phys. Rev. **89**, 1202 (1953).

the various types of metastable–metastable collisions. This leads to $\sigma_{3s-3s}=1.14\times10^{-14}$ cm^2.

The rate coefficient for collisions between pairs of $3s$ state atoms is given by $\alpha_S=\sigma_{3s-3s}\bar{v}_R$, where $\bar{v}_R$ is the mean relative velocity of the two colliding particles. For neon at 573°K, this leads to $\alpha_S=1.248\times10^{-9}$ cm^3/sec.

VI. DETERMINATION OF THE PREDOMINANT IONIZATION MECHANISM

With numerical estimates for the various reaction rates, it is now possible to determine the excited atom density using Eqs. (6) and (7). Evaluation of the terms in Eq. (7) yields $b[(D_M/\Lambda_1^2)+\gamma_M N^2]=575$ sec^{-1} and $(1-b)\nu_{IR}=2.11\times10^4$ sec^{-1}. The peak value of $Z_E(z)$ attained in Fig. 7 is 375 sec^{-1}. Thus, it is seen that the decay of imprisoned resonance radiation far surpasses both diffusion of metastable atoms and electron-impact ionization of excited atoms in importance as a loss mechanism. Substitution of the derived values of the various reaction rates into Eq. (6) then leads to the spatial variation along the z axis of $n^*(z)$ shown in Fig. 8.

Knowing $n^*(z)$, it is possible to determine the rates of generation of ions by various mechanisms involving the $3s$ states. The rate of ionization of $3s$ state atoms by electron impact is given by $H_E(z)=Z_E(z)n^*(z)$ using the data from Figs. 7 and 8. The rate of generation of ions by collisions between pairs of $3s$ state-excited atoms is given by $H_G(z)=-H_F(z)=\alpha_S[n^*(z)]^2$. The results of these computations are shown in Fig. 9, where the rate of ionization of ground-state atoms by electron impact, $H_I(z)$, is also presented. $H_I(z)$ was computed using the Martin and Rowe[12] data (Fig. 1) for $n^-(z)$ and $T^-(z)$ and the latest published data for the ionization cross section.[28] The relative importance of the various processes may be determined by comparing the areas under the curves in Fig. 9. It is found that 76% of the ions in the discharge are produced in collisions between pairs of excited atoms, while 23% of the ions are produced by direct ionization of ground-state atoms. At most, 1% is due to two-stage electron-impact ionization. The curves for H_I and H_G in Fig. 9 are therefore nearly equal to the spatial rates of generation of atomic and molecular ions, respectively.

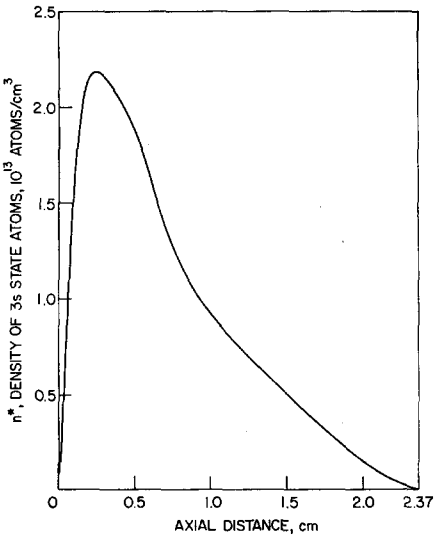

FIG. 8. Axial variation of the density of excited atoms in the $3s$ configuration.

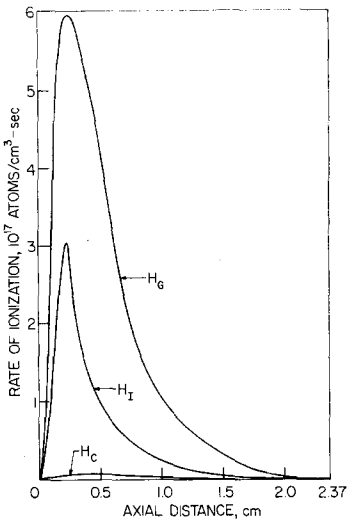

FIG. 9. Axial variation of the ionization rates for the ionization mechanisms under consideration.

With a knowledge of the relative rates of generation of atomic and molecular ions, their relative concentrations in the discharge can be determined. Extrapolation of published data[29] indicates that at 573°K the mobilities of atomic and molecular ions in neon are nearly equal, and since their spatial rates of generation and mobilities are very similar, the spatial distributions of the densities of the two species will aso be very similar. Molecular ions are also subject to loss by dissociative recombination, and this will tend to decrease the molecular ion density somewhat. Consequently, based upon the relative rates of generation of the two species, it is estimated that the density of molecular ions in the neon low-voltage arc dominates the density of atomic ions by a factor of between 2:1 and 3:1.

VII. RELATIVE IMPORTANCE OF THE VARIOUS LOSS MECHANISMS

By conservation of energy, the sum of the power inputs to the discharge must equal the sum of the power losses. Thus,

$$[V_aI]+[\Phi_cI+(2kT_c/e)I]=[\Phi_aI+(2kT_e(d)/e)I]+W_{\text{ion}}+W_{\text{ex}}+W_{\text{rad}}+W_{\text{rec}}. \quad (13)$$

Here, V_a is the applied voltage, Φ_c and Φ_a are cathode

[28] D. Rapp and P. Englander-Golden, J. Chem. Phys. **43**, 1464 (1965).

[29] L. M. Chanin and M. A. Biondi, Phys. Rev. **106**, 473 (1957).

and anode work functions, T_c is the cathode temperature, and $T_e(d)$ is the electron temperature just outside the anode. The first term on the left is the electrical input power from the dc supply, while the second term on the left is the electron emission cooling of the cathode, which must be supplied by the cathode heater supply. The first term on the right is the power delivered to the anode by the plasma electrons. The remaining power losses are: W_{ion} due to direct ionization of ground state atoms; W_{ex} due to excitation of atoms to the $3s$ configuration and the subsequent losses from this configuration by various mechanisms; W_{rad}, due to the escape of radiation from $3p\rightarrow 3s$ transitions; and W_{rec}, due to recombination.

For the conditions $V_a=10.7$ V, $I=4$ A, $T_c=1100°$C, $\Phi_c=1.6$ eV, and $\Phi_a=4.2$ eV obtained from Martin and Rowe,[12] Eq. (13) yields $V_aI=42.8$ W and $(\Phi_c+2kT_c/e)I=7.3$ W. Thus, in the present case, the thermionic input power is small compared with the electrical input power.

Also from the data of Martin and Rowe, $kT_e(d)$ is taken as 1.75 eV. The power delivered to the anode by the plasma electrons is then $\Phi_aI+[2kT_e(d)/e]I=30.8$ W.

To estimate W_{ion}, assume that the spatial rate of ionization varies approximately exponentially and at a uniform rate in the radial direction, so that $H_I(z,r)\cong H_I(z)\exp(-r/\bar{r})$. Since H_I is proportional to the electron density $\bar{r}$ is taken as the radial distance at which $n_e^-(z,r)=(1/e)n_e(z,0)$. W_{ion} is then given by

$$W_{\text{ion}}=2\pi\bar{r}^2\mathcal{E}_I\int_0^d H_I(z)\,dz.$$

From Fig. 2, it is estimated that $\bar{r}\cong 0.8$ cm. Graphical integration of $H_I(z)$ in Fig. 9 then gives $W_{\text{ion}}=1.5$ W.

The power expended in exciting atoms to the $3s$ configuration may be estimated in the same manner. Use of the average energy of the $3s$ states, $\mathcal{E}_{3s}$, and graphical integration of Fig. 6 yields $W_{\text{ex}}=17.9$ W. This power is shared among the various losses from the $3s$ configuration. Of these, the losses due to the deexcitation of metastables in three-body collisions and due to the electron-impact ionization of $3s$ atoms have been found negligible. The power expended in collisions between $3s$ excited atoms is found by graphical integration of $H_G(z)$ in Fig. 9, noting that the total energy of the colliding atoms is $2\mathcal{E}_{3s}$. This yields 8.0 W. The energy required for formation of a molecular ion is $\mathcal{E}_I-\mathcal{E}_{\text{bind}}$, where $\mathcal{E}_{\text{bind}}$ is the binding energy of the molecular ion. For Ne_2^+, $\mathcal{E}_I-\mathcal{E}_{\text{bind}}=20.2$ eV and the total potential energy of the two colliding atoms is 33.4 eV. The net power expended in producing the molecular ions is then $(20.2/33.4)8.0=4.8$ W. The remaining 3.2 W goes into internal energy of the ions and the kinetic energy of the ejected electrons. Finally, it is found that 9.6 W are lost by the escape of resonance radiation and only 0.3 W is lost by the diffusion of metastable atoms.

The power loss due to dissociative recombination of molecular ions is

$$W_{\text{rec}}=\mathcal{E}_{\text{bind}}\alpha_R F_M\int_0^d dz\int_0^\infty dr\cdot 2\pi r[n_e(z,r)]^2.$$

Here α_R is the dissociative recombination coefficient and F_M is the fraction of ions that are molecular. As before, $n_e(z,r)$ is taken to be of the form $n_e(z,r)=n_e(z,0)\times\exp(-r/\bar{r})$. The latest available data gives[30] $\alpha_R=2.2\times10^{-7}$ cm^3 sec^{-1}. Also, $\mathcal{E}_{\text{bind}}=1.4$ eV, $\bar{r}$ is taken as 0.8 cm, and F_M is taken as 0.75. Graphical integration of $[n_e(z,0)]^2$, obtained from Fig. 1, then gives $W_{\text{rec}}=0.5$ W.

The power loss due to the escape of radiation from $3p\rightarrow 3s$ transitions (neon red light) cannot be directly calculated because of a lack of reliable data for the excitation cross sections for $3s\rightarrow 3p$ transitions. Instead, W_{rad} is determined by substituting the computed values of the other generation and loss mechanisms into Eq. (13) and solving for W_{rad}. This yields $W_{\text{rad}}\cong 0.3$ W. Thus, this loss mechanism is relatively unimportant.

VIII. CLOSURE

On the basis of the present analysis several conclusions may be drawn concerning the nature of the excitation, ionization and loss mechanisms in the low-voltage arc mode of a neon plasma diode. First, in contrast to the low-voltage arc mode in cesium plasma diodes, the neon low-voltage arc is not in a state of quasi-equilibrium. Consequently, multistage cumulative ionization involving the many excited states of neon is not of significance in the neon low-voltage arc. Neither is three-body recombination of importance as a loss mechanism.

Atoms in the $3s$ resonance and metastable states are found to play an important role in governing the behavior of the discharge. Most of the resonance and metastable-state atoms are generated in a region near, but separated from, the cathode. This region corresponds to the intensely illuminated "cathode ball-of-fire" region of the low-voltage arc mode. The results indicate that the nonuniform excitation arises primarily from the high-energy tail of a spatially varying quasi-Maxwellian electron-energy distribution, rather than from primary electrons accelerated through the cathode double sheath. Relatively slow rates of metastable atom diffusion and escape of imprisoned resonance radiation keep the density of excited atoms quite high in the primary generation region.

The cross section for collisions between excited atoms was found to be quite large ($\simeq 10^{-14}$ cm^2) and it was shown that there is an overwhelming probability that such a collision results in the formation of a molecular

[30] H. J. Oskam and V. R. Mittelstadt, Phys. Rev. **132**, 1445 (1963).

ion. It was found that this process accounts for roughly three fourths of the ions generated. The remainder are atomic ions produced by direct ionization of ground-state atoms by electrons in the high-energy tail of the thermalized distribution. Two-stage electron-impact ionization was found to be negligible.

[By considering the various loss mechanisms for the two ionic species, it was estimated that in the neon low-voltage arc, molecular ions are more numerous than atomic ions by a factor of between 2:1 and 3:1.

The authors appreciate the reviewer calling their attention to the relevant experimental work of Weimar and Pahl[31–33] on the subject. These experimenters studied noble-gas discharges in the pressure range of 0.1–5 Torr by effusing ions of the discharge through a small hole in the chamber and then studying them with a mass spectrometer. The fraction of molecular ions was found to increase with increasing pressure, reaching 15% in helium and neon and 40% in argon. These experimental results reinforce the above conclusions.]

In considering the power losses in the discharge, it was found that 62% of the input power was delivered to the anode by the plasma electrons. The escape of resonance radiation accounted for 19% of the total power loss, while ionization by all mechanisms accounted for 13%. The losses due to the dissociative recombination of molecular ions, the diffusion of metastable atoms, and the emission of neon red light were the least important of the mechanisms considered.

[31] M. Pahl and U. Weimer, Z. Naturforsch. **13a**, 745 (1958).
[32] Ref. 31, p. 753.
[33] M. Pahl, Z. Naturforsch. **14a**, 239 (1959).

JOURNAL OF APPLIED PHYSICS VOLUME 39, NUMBER 9 AUGUST 1968

Effect of Heat Treatment on the 1.370 eV Photoluminescence Emission Band in Zn-Doped GaAs

C. J. HWANG
Bell Telephone Laboratories, Incorporated, Murray Hill, New Jersey
(Received 25 January 1968; in final form 15 April 1968)

A number of changes in the 1.370 eV photoluminescence band are observed in Zn-doped GaAs after heat treatment in molten KCN, Ga, or diffusion with Cu at temperatures ranging from 235° to 1100°C. The band is replaced by a Cu_{Ga}^{-} band at 1.356 eV after Cu diffusion under intrinsic conditions and can be eliminated or preserved, respectively, by heat treating the crystal in molten KCN or Ga above 650°C. Emission of a broad band near 1.37 eV with a sharp-line structure appears after saturation with Cu at temperatures between 550° and 370°C. The structure has a zero-phonon line at 1.429 eV and additional lines separated by about 0.011 eV. No change in the shape of the 1.370 eV band is seen for heat treatment below 550°C in the absence of copper. It is proposed that the centers associated with the 1.370 eV band are $V_{As}Zn_{Ga}$ or $D_{As}Zn_{Ga}$ pairs, where V_{As} and D_{As} denote an As vacancy and a donor impurity occupying an As site, and that the centers responsible for the band with sharp-line structure are $V_{As}Cu_{Ga}$ or $D_{As}Cu_{Ga}$ pairs. The sharp-line structure probably involves emission of local-mode phonons resulting from the pair substituting for a Ga–As pair in the crystal.

I. INTRODUCTION

Broad-band emission at 1.370 eV, in addition to the near gap emission at 1.485 eV, has been previously observed in melt-grown Zn-doped GaAs crystals.[1] However, the specific defects giving rise to this band were unknown. It was suggested earlier that this broad band is caused by transitions involving native defects since it disappears or diminishes in intensity after heat treatment above 600°C.[1]

The present work investigates the nature of the defect responsible for the 1.370 eV band by studying the effect of heat treatment. In this study heat treatment is performed over a wide range of temperatures (235° to 1100°C) under several annealing conditions (molten KCN and Ga treatment, and Cu diffusion). KCN is used to prevent diffusion of external contaminating impurities into the crystal.[2] Saturation with Ga is used to control the arsenic vacancies. Cu diffusion can reveal information about the nature of the defect because of its relative ease of reaction with the defect.

II. EXPERIMENTAL

A Bridgman crystal with hole concentration of about 4×10^{16} cm^{-3} was chosen for this work, for crystals of this doping sometimes exhibit stronger emission at 1.370 eV than at 1.485 eV. A low-doped crystal also avoids the interference of the second phonon replica of the 1.485 eV band with the 1.370 eV band.

Heat treatment was carried out in sealed quartz ampoules evacuated to about 5×10^{-6} Torr. For heat treatment without copper, the sample was either immersed in molten KCN[2] or placed in a high-purity

[1] C. J. Hwang, J. Appl. Phys. **38**, 4811 (1967).
[2] J. Blanc and L. R. Weisberg, J. Phys. Chem. Solids **25**, 221 (1964).